Temporal encoded orientation maps with CBV-weighted fMRI in primary visual cortex.

C. Moon[1], H. Fukuda[1], S-G. Kim[1]

[1]Dept. of Neurobiology, Pittsburgh, PA, United States

[Introduction] Mapping functional columns with conventional blood oxygenation-level dependent (BOLD) fMRI has been successfully performed on the ocular dominance column in humans [1-5]. Also, the orientation column has been mapped in anesthetized cats using early negative BOLD [6], cerebral blood flow (CBF)-based [7] and cerebral blood volume (CBV)-weighted fMRI [8]. Although these fMRI maps have the appearance of functional columns, the maps have not been evaluated by other well-established recording methods such as electrophysiological recording or optical intrinsic signal (OIS) imaging. Thus, the validity of fMRI column maps is still questionable. In the present study, we compared orientation column maps of CBV-weighted fMRI with the contrast agent monocrystalline iron oxide nanoparticle (MION) to those of OIS imaging in the same cat. The choice of CBV-weighted fMRI with MION was because only this method satisfied both sensitivity and specificity for functional column mapping as well as being easy to implement [8]. To further improve the sensitivity for orientation-specific signal we also adopted temporally-encoded methods in the stimulation paradigm and Fourier analysis [9, 10] instead of the conventional block design stimulation [1-8]. The spatial vessel information of the 3-D venogram was used to select a precise slice after considering any large vessel artifacts, and the orientation columns perpendicular to that imaging slice.

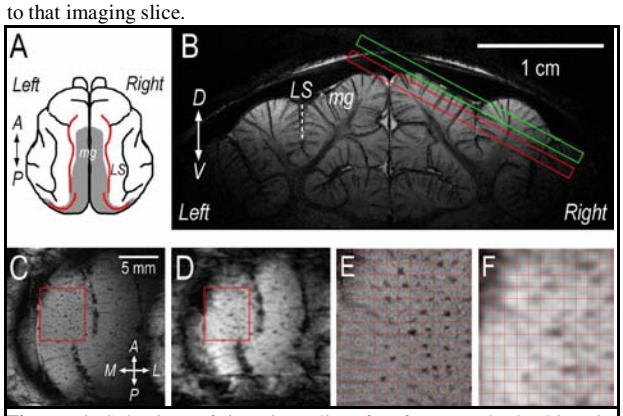

Figure 1 Selection of imaging slice for fMRI and checking its distortion. ***A***, A schematic dorsal view of the cat brain. ***B***, A coronal view of a 2-D venographic image. The red rectangle is the slice position for fMRI and the green one is for the pial vessel image. ***C***, T2*-weighted image is obtained from the oblique plane shown in *B*, red box. ***D***, An fMRI EPI image at the same plane in *C*. In *C* and *D*, red boxes are the region of interest to be compared with OIS and locally shimmed. ***E*** and ***F***, The boxes on the images *C* and *D* are enlarged for detail comparison, respectively. Grids are 0.5 mm x 0.5 mm. In *A- C*, Abbreviations: *LS*, lateral sulcus; *mg*, marginal gyrus; *A*, anterior; *P*, posterior; *M*, medial; *L*, lateral; *D*, dorsal; *V*, ventral.

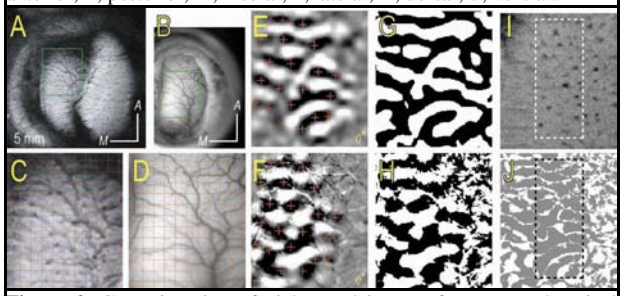

Figure 2. Co-registration of pial vessel images for MRI and optical imaging. ***A***, Pial vessel patterns above the fMRI slice (green box in Figure 1B). ***B***, OIS pial vessel patterns above the MRI slice of *A*. ***C*** and ***D***, The regions of the green box (5.8 mm x 6.5 mm) on images *A* and *B* are enlarged for detail comparison, respectively. Grids are 0.5 mm x 0.5 mm. ***E*** and ***F***, Iso-orientation maps of 0° from fMRI and OIS after the pial vessel co-registration. ***G*** and ***H***, Binary images of *E* and *F*, respectively. ***I***, A T2*-weighted anatomical image in the co-registered region. The dotted rectangle indicates a region to be quantitatively compared. ***J***, Overlapped area between images *G* and *H* is colored in gray. The position of the dotted rectangle is the same as with *I*. *A*- B, Abbreviations: *A*, anterior; *M*, medial.

[Methods] Stimulus orientation-specific activation in the primary visual cortex (Fig. 1A, shaded area) was measured with CBV-weighted fMRI (n = 6) and OIS imaging (n = 3 of 6) sequentially in the same anesthetized cat. The identical continuous visual stimulation was used in both measurements: high-contrast full-field moving gratings of eight orientations (10 s each) cycled ten times (i.e., a total of 800-s stimulation presentation). The continuous stimulation increased the power of the orientation-specific frequency signal, while suppressing non-specific signals, especially from large veins. CBV-weighted fMRI with MION (10mg/kg) was performed on an area of 2x2-cm^2 parallel to marginal gyrus of one hemisphere at 9.4T/31cm horizontal magnet (Varian, CA) using navigator-echo corrected four-segmented GE EPI sequence (TR/TE=2s/10ms). A total of 400 images were continuously acquired during the 800-s stimulus presentation. An imaging slice (128x128 pixels, 1mm thick.) was positioned ~0.5 mm below the pial mater to avoid artifacts from large pial vessels (Fig. 1B, red rectangle). A pial vascular pattern above the imaging slice was also obtained for later image co-registration (Fig. 1B, green rectangle). The position of the slices was determined using 3-D venogram (TR/TE=20/50ms, matrix=512x256x256, FOV=3.5x1.6x2.0cm^3) [11]. For the anatomical reference image for functional studies, the conventional T_2*-weighted gradient echo was also used (Fig. 1C). Following fMRI experiments, CBV-weighted OIS imaging was performed above the MR imaging slice using the custom-made real-time imaging system [12]. To obtain CBV-weighted OIS, the wavelength of 570 nm (i.e., a hemoglobin iso-sbestic point) was used for the cortical illumination. The image (18.5 x 13.9mm^2, 28.9 μm / pixel) was acquired every 1/30s during the 800-s recording time (a total of 24000 images). For the analysis of data, the frequency component at the orientation-specific stimulation cycle (1/80 s) was extracted from the time series data on a pixel-by-pixel basis to obtain iso-orientation maps [9, 10]. To quantify similarity between the two co-registered maps, each map was first binarized (Fig. 2G and H) and overlapped area was then determined (Fig. 2J) by dark spots (these emerging veins are perpendicular to the imaging plane in this tangential area (Fig. 2I)) to minimize the intrinsic error between two modalities due to the slice-deterministic (fMRI) and projection (OIS) characteristics.

[Results and Conclusion] EPI images for functional studies (Fig. 1D) were compared to the anatomical image to examine minimal distortion of EPI (Fig. 1 E and F). As in the panels, the centers of individual emerging veins (dark spots) did not change between the anatomical and EPI image, suggesting negligible image distortion. The CBV-weighted fMRI combined with the temporally-encoded continuous stimulation method provided a clear orientation column fMRI map (see Fig. 2E) at only orientation-specific stimulation frequency (1/80 s). The reproducibility of the maps between two different 800-s sessions was significantly high for all six cats ($P < 0.001$); the average correlation coefficient between two maps on pixel-by-pixel comparison was $R = 0.77 \pm 0.09$ (Mean ± SD, n = 6). In order to compare fMRI with optical imaging, pial vessel patterns from MRI and optical imaging (Fig. 2A and B) were co-registrated. Then, fMRI and OIS images were compared (Fig 2E vs. 2F). Dark regions in both functional images indicate sites preferentially responding to 0° orientation, while white regions are corresponding to 90° orientation-selective domains. The fMRI iso-orientation columns were well co-localized to the OIS columns (Fig. 2E and F). The average percentage of the column overlap between two maps was 70.5 ± 2.67 (%) (Mean ± SD, n=3). This suggests that the CBV-weighted fMRI response is well localized to the site of neural activity. Since we confirmed the validity of the fMRI map, CBV-weighted fMRI can be used for mapping functional structures in the brain regions in which OIS imaging cannot be applied.

[Reference] **1**. Goodyear, B. G. et al., *Hum Brain Mapp 14:* 210-7 (2001). **2**. Menon, R. S., et al., *J Neurophysiol 77:* 2780-7 (1997). **3**. Cheng, K. et al., *Neuron 32:* 359-74 (2001). **4**. Menon, R. S. et al., *Magn Reson Med 41:* 230-5 (1999). **5**. Dechent, P. et al., J. *Neuroreport 11:* 3247-9 (2000). **6**. Kim, D. S. et al., *Nat Neurosci 3:* 164-9 (2000). **7**. Duong, T. Q. et al., *Proc Natl Acad Sci U S A 98:* 10904-9 (2001). **8**. Zhao, F. et al., *Neuroimage 27:* 416-24 (2005). **9**. Kalatsky, V. A. et al., *Neuron 38:* 529-45 (2003). **10**. Engel, S. A. et al., *Cereb Cortex 7:* 181-92 (1997). **11**. Park, S.H. et at. *ISMRM*, 1718, (2005). **12**. Moon, C.H. et al., 33th *SfN*, (2004).

[Acknowledgements] We thank Sung-Hong Park for MR venography and Michelle Tasker for animal preparation. Supported by NIH NS44589 & EB003324.